Chapter

Confocal Laser Scanning Microscopy for Spectroscopic Studies of Living Photosynthetic Cells

Natalia Grigoryeva and Ludmila Chistyakova

Abstract

Self-fluorescence of light-harvesting complex is a powerful tool for investigation of living photosynthetic microorganisms. As the physiological state of single cells of such microorganisms is closely related to the operation and activity of photosynthetic system, any variations in spectroscopic properties of their self-fluorescence indicate the changes in their physiological state. In this chapter, we present several applications of confocal laser scanning microscopy (CLSM) for investigation of living photosynthetic cells. A set of ordinary CLSM techniques will be applied for studying of cyanobacteria (or blue-green algae) such as 3D imaging, spectral imaging, microscopic spectroscopy, and fluorescence recovery after photobleaching (FRAP). Cyanobacteria were chosen as a model microorganism due to their great importance for different scientific and biotechnological applications. Cyanobacteria are the most ancient photosynthetic microorganisms on Earth. Nowadays, cyanobacteria are one of the most wide-spreaded organisms in nature, and the ecological aspect in their investigation is quite valuable. On the other hand, thousand strains belonging to different species are cultivated in biolaboratories all over the world for different biotechnological applications such as biofuel cells, food production, pharmaceuticals, fertilizers, etc. Thus, the noninvasive spectroscopic methods are quite important for monitoring of physiological state of cyanobacterial cultures and other photosynthetic microorganisms.

Keywords: confocal laser scanning microscopy, fluorescent microscopic spectroscopy, spectral imaging, 3D bio-imaging, cyanobacteria, blue-green algae, photosynthetic system, photoactive pigment, light-harvesting complex

1. Introduction

Confocal laser scanning microscopes (CLSMs) are distinguished by their high spatial and temporal resolution [1, 2]. Modern laser scanning microscopes are unique tools for visualizing cellular structures and analyzing dynamic processes inside single cells. They exceed classical light microscopes especially in their axial resolution, which enables to acquire optical sections (slices) of a specimen. An object can thus be imaged completely in three dimensions and subsequently visualized as a 3D computer image. Apart from simple imaging, confocal laser scanning microscopes are designed for the quantification and analysis of image-coded

information. Among other things, they allow easy determination of fluorescence intensities, distances, areas, and their changes over time. In particular, they are capable of quickly detecting and quantitatively unmixing the spectral signatures of fluorescent objects. Many software functions analyze important parameters such as the degree of colocalization of labeled structures, or the ion concentration in a specimen. New acquisition CLSM tools include the detection of quantitative properties of the emitted light such as spectral signatures and fluorescence lifetimes. The most impressive feature of modern CLSMs is their capability for single-cell microscopic spectroscopy, which allows to obtain spectroscopic information inside single cells and small regions. Another group of applications is the quantitative investigations of dynamic processes in living cells using techniques such as fluorescence recovery after photobleaching (FRAP), fluorescence resonance energy transfer (FRET), photoactivation, and photoconversion.

The specific field of CLSM application is the investigation of self-fluorescence of living cells. The conventional biological fluorescent studies are based mostly on using fluorescent dyes and labels (chromophores). But it is well-known that the fluorescent dyes, even most flexible, affect living cells considerably. Thus self-fluorescence should become the most suitable tool for noninvasive investigation of changes in physiological state of living cells. For instance, the photosynthesis research employs the detection of self-fluorescence as a key method to study the metabolic mechanisms in photosynthetic cells and to detect photosynthetic efficiency in vivo. Recent rapid development of confocal microscopes functionality initiates new directions in subcellular biology research. However, the experiments with photosynthetic cells require some additional specific skills and techniques to perform measurements and to carry out data processing [3–7]. The efficiency of photosynthesis and photosynthetic rate are highly dependent on irradiance. This can be seen in the light-dependency of various photosynthetic parameters [8]. Moreover, not only light quantity, but also light "quality" (wavelength) is an important factor. Thus, special spectroscopic methods are required to study the physiology of phototrophic microorganisms [9]. These organisms employ light-dependent photosynthesis as the main energy source for their metabolism and the detected self-fluorescence finally reflects the diversity in morphological and physiological states of their photosynthetic cells [3–7].

CLSM single-cell microscopic spectroscopy is undoubtedly the most powerful tool for in vivo investigation of physiological processes in photosynthetic organisms (cyanobacteria, algae, and higher plants). The investigation of self-fluorescence of single living cells reveals the relation between the physiological state and the operational activity of photosynthetic system. A lot of interesting static and dynamic effects can be studied by means of confocal laser scanning microscopy. The investigation of self-fluorescence gives the information about single-cell processes as well as about the collaboration in cell communities. Changes in spectral characteristics of living photosynthetic cells indicate changes in their physiological state and can be applied for the studies of the results of stress states and external actions.

Recent progress in confocal laser scanning microscopy (CLSM) gives an opportunity to investigate different physiological processes in photosynthetic organisms on a single-cell level. Such CLSM applications as spectral unmixing and lambda-scanning provide the recording of spectral characteristics from living cells. FRAP and FLIP applications allow to study dynamic processes such as cell membrane fluidity and phycobilisome diffusion along thylakoid membrane. The nondestructive spectroscopic analysis conducting in vivo at a sub-cellular level allows to obtain more complete information about special features of individual cyanobacterial cells and supports the registration of very weak variations in their physiological state. For example, a novel technique for discrimination of cyanobacterial species and physiological states of the cells belonging to one strain was elaborated by the

authors of the present chapter [3–5]. The technique is based on a strict relation between physiological state and genera affiliation of cyanobacterial cells and the intensity and the shape of corresponding single-cell fluorescence spectra, obtained by means of confocal microscopic spectroscopy. Light-, heat-, ultrasound- and toxin-induced changes can be distinguished by means of confocal microscopic spectroscopy since all these external actions are stress factors affecting photosynthetic process [5]. The application of such techniques for automation of on-line monitoring will give an additional opportunity to rise an effectiveness of biotechnological production and will bring in a valuable contribution to the development of innovative approaches in environmental monitoring [4, 5].

Here we present several experimental approaches to study the metabolic mechanisms in single photosynthetic cells in vivo. They are accompanied by several examples of in vivo investigations. Three main CLSM tools will be discussed in details: spectral imaging, fluorescent microscopic spectroscopy, and FRAP. All presented results were obtained using cyanobacterial strains from CALU collection of the Core Facility Center "Centre for Culture Collection of Microorganisms" of the Science Park of St. Petersburg State University as a model objects for CLSM studies.

2. Natural fluorescence

Opposite to the absorption spectra, the in vivo fluorescence spectra are much more informative. Fluorescence detection is a powerful tool owing to the existence of natural fluorescence from phycobilins and chlorophylls. It is a highly sensitive, nearly instantaneous, noninvasive way to study various components and processes in situ and in vivo. Although the fluorescence spectra contain the information only about photosynthetic apparatus of different algal groups, they include the information about the chemical structure of light harvesting complex (LHC) and accessory pigment-proteins, as well as about the character of links between pigment-protein complexes and the efficiency of energy transfer in the light harvesting process. When compared with absorption, fluorescence is affected by the excitation wavelength and energy. Thus, the use of different excitation wavelengths can provide more detailed information for the study of single-cell composition.

Today, there is no doubt that the in vivo analysis of fluorescence parameters of light-harvesting complexes is a powerful tool for studying the effect of a wide variety of environmental factors on photosynthetic organisms. The intensity of fluorescence emitted by single photosynthetic cells in vivo depends on the structure and operational effectiveness of photosynthetic apparatus, reflecting the individual characteristic of cyanobacterial strain and in-time physiological state of the cells under consideration. The environmental changes cause the changes in bioenergetic processes occurring in cyanobacterial cells, and so they significantly affect the kinetics parameters and spectral features of the intrinsic fluorescence of photosynthetic apparatus. Thus, the intrinsic fluorescence spectra of a particular type of cyanobacteria, the so-called "fluorescent fingerprints", can be used to identify photosynthetic pigments and to determine the viability of individual cells. These "fluorescent fingerprints" can be easily obtained by the routine lambda-scanning at most of confocal laser scanning microscopes.

2.1 Model object

Cyanobacteria, used in this study as a model object, are photoautotrophic prokaryotes. They are important microorganisms that contributed to the early oxygenation of the atmosphere and oceans on Earth 3.5 billion years ago. Now, cyanobacteria species are

widely spreaded in nature and different morphologies with unicellular and filamentous forms can be found among them (**Figure 1**). Cyanobacteria as oxygen-evolving photosynthetic prokaryotes are good candidates for being a suitable system for numerous biological applications. Cyanobacteria have special metabolic features of autotrophic carbon and nitrogen assimilation and energy supply via photosynthesis, which presents an increased potential for the next generation of sustainable bioproduction.

In the last years, the investigation of taxonomy, physiology, morphology, and genetics of cyanobacteria attracts a considerable attention due to their potential application in biotechnology [10–16] and biosensing [17–19]. Cyanobacterial hydrogen has been considered as a very promising source of alternative energy and has now been made commercially available. Cyanobacteria are also used in aquaculture, wastewater treatment, food, fertilizers, agriculture, and production of secondary metabolites including exopolysaccharides, vitamins, toxins, enzymes, and pharmaceuticals. In addition, the ecological aspect of the harmful bloom monitoring and control makes an important contribution to this rising interest to cyanobacterial problem. A vast amount of different techniques were elaborated to achieve a nowadays insight of the physiological processes that rules cyanobacterial life and their genetic background.

As far as cyanobacteria are ancient photosynthetic microorganisms, they have complex and effective light harvesting apparatus, which exhibit multifarious self-fluorescent properties. These intrinsic natural features are essential for fluorescent non-destructive analysis on a single-cell level and give a unique opportunity for steady-state and time-resolved investigations of various physiological processes in vivo.

In these studies, several cyanobacterial strains from CALU collection of the Core Facility Center "Centre for Culture Collection of Microorganisms" of the Science Park of St. Petersburg State University were utilized.

Before the investigations were carried out, the cyanobacterial cells were cultivated during 7 days in BG 11 medium (at 28°C) under continuous white light irradiation (fluorescent tubes, 40 μmol photons/m^2/s). The cyanobacterial cells for visualization were taken at stationary phase of growth. For CLSM imaging, the

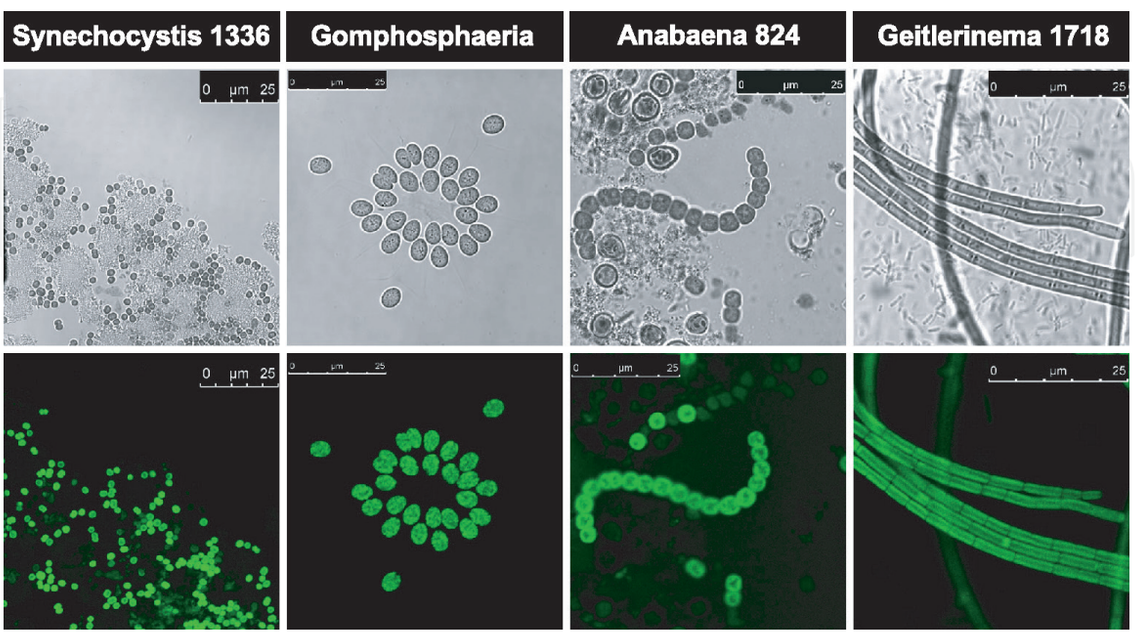

Figure 1.
Confocal laser scanning photomicrographs illustrating the morphological features and biological diversity of free-living and laboratory cyanobacterial strains: Synechocystis CALU 1336, Gomphosphaeria (wild type), Anabaena CALU 824, and Geitlerinema CALU 1718. Both fluorescence and transmission photomicrographs are presented. The white bar corresponds to 25 μm.

living cells were placed onto a glass slide and were allowed to settle. A glass coverslip was placed on top and sealed with nail polish. Samples were immediately imaged. All studies were performed with living cells at room temperature. Note here, that any centrifugation and/or resuspending of cyanobacterial cultures before microscopic measurements change considerably the physiological state of cells under consideration, and thus should be eliminated.

2.2 Light-harvesting system

Photosynthetic system of cyanobacteria, in contrast to higher plants, contains the external membrane light-harvesting complexes. Their antenna complex for photosystem II (PS II), and to some extent for photosystem I (PS I), is extrinsic and formed as a large multiprotein organelles, which are located on the stromal side of the thylakoid membranes. These supramolecular pigment-protein complexes are called phycobilisomes (PBSs). The detailed description of the morphology, structure, chemical, and optical properties of light-harvesting complex of cyanobacteria, phycobilisomes, and detached phycobilins can be found in numerous publications [8, 20–34]. Here, we only pointed out several main features that were essential for further discussion.

The main accessory pigments in cyanobacteria are phycobilins. The phycobilins which are bounded to proteins are known as phycobiliproteins. The three classes of phycobiliproteins in antenna complexes are allophycocyanin, phycocyanin, and phycoerythrin. However, in some cyanobacteria, phycoerythrin can be replaced by phycoerythrocyanin or both pigments can be lacking; phycocyanin and allophycocyanin are constitutively present in all cyanobacteria.

PBSs are assembled from 12 to 18 different types of polypeptides which may be grouped into three classes: (1) phycobiliproteins, (2) linker polypeptides, and (3) PBS-associated proteins. Phycobiliproteins, a colored family of water-soluble proteins bearing covalently attached, open-chain tetrapyrroles known as phycobilins. On the other hand, most of linker polypeptides do not bear chromophores.

Phycobilisomes are constructed from two main structural elements: a core substructure and peripheral rods that are arranged in a hemidiscoidal fashion around that core (**Figure 2**). The core of most hemidiscoidal phycobilisomes is composed of three (or two) cylindrical subassemblies, which are arranged side-by-side and form a triangle stack. Each core cylinder is made up of four disc-shaped phycobiliprotein trimmers, allophycocyanin (APC), allophycocyanin B (APC-B), and APC core-membrane linker complex (APC-LCM). By the core-membrane linkers, PBSs are attached on thylakoids and structurally coupled with PSII. The peripheral cylindrical rods (six or eight) radiate from the lateral surfaces of the core substructure and are usually not in contact with the thylakoid membrane. The rods are made up of hexamers, disc-shaped phycobiliproteins, phycoerythrin (PE), phycoerythrocyanin (PEC) and phycocyanin (PC), and corresponding rod linker polypeptides [8, 24–26, 32–35].

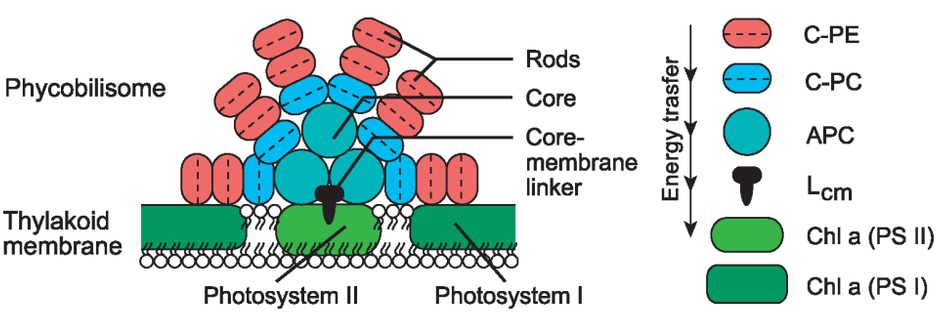

Figure 2.
Schematic drawing of a phycobilisome and the photosynthetic energy transfer to the reaction center.

2.3 Absorption, fluorescence, and energy transfer

As it was mentioned above, the fluorescence is one of the most powerful ways to probe photosynthetic systems, because it reports on the energy transfer and trapping. The intrinsic fluorescence of photosynthetic organisms originates from excited states that were trapped by light-harvesting system and lost before photochemistry took place.

In the light-harvesting pigment-protein complexes of cyanobacteria, the pigment molecules are excited by photons. In a nonradiating-induced resonance transfer process leading up to the reaction centers, they transfer the excitation energy to other pigment molecules which are excited in turn. In phycobilisomes, this fast process has an efficiency of almost 100%.

There are two mechanisms that serve the efficient excitation transfer in the light harvesting complex of cyanobacteria: the inductive resonance (Förster) transfer, applicable at long distances and weak interactions, and the occurrence of delocalized excitons, applicable at short distances and strong interactions [26].

The most likely mechanism by which excitation hops from one pigment complex to another across distances greater than several Angstroms is inductive resonance transfer, also known as Förster transfer [36, 37]. The interaction between an electronically excited pigment and its unexcited neighbors results in a downward transition of the initially excited group coupled with an upward transition in the nearby acceptor pigment by a through space Coulombic interaction (**Figure 3**). The energy donor and energy acceptor molecules must have an energy state in common, because when the excitation hops from donor to acceptor, the conservation of energy is required. This can be so only if the two molecules have a common energy state and therefore spectral transitions at the same wavelength. It should be noted, that the requirement for overlap of the fluorescence emission spectrum of the donor and the absorption spectrum of the acceptor does not lead to the process of emission of a photon by the donor, which is followed by absorption of a photon by the acceptor. The Förster transfer is a nonradiative process, which means that no photon emission or absorption is involved.

A critical step in the energy storage process is energy transfer between the antenna and the reaction center, where separation of the electron from a positively charged hole occurs. The molecules that accomplish the last event are organized in the photosynthetic membranes in a highly specific fashion to achieve the high efficiency of light energy conversion to photochemistry [30, 38].

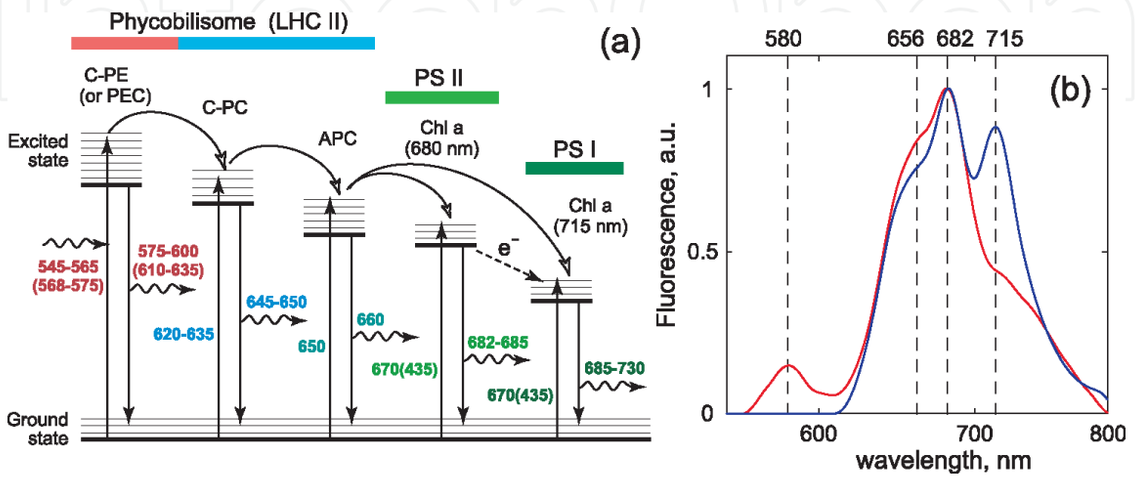

Figure 3.
Schematic illustration of the energy transfer in light-harvesting system of cyanobacteria (a). Panel (b) represents the normalized in vivo single-cell fluorescence emission spectra of two cyanobacterial species: blue line—Leptolyngbia CALU 1713 and red line—Nostoc CALU 1817. Excitation wavelength 488 nm. Dashed lines and numbers over them indicate emission wavelengths of PE, PC, and Chl a of PCII and PCI, correspondingly.

The more distal parts of the antenna system, often a peripheral antenna complex (phycobilisome), maximally absorb photons at shorter wavelengths (higher energies) than do the pigments in the antenna complexes that are proximal to the reaction center. Subsequent energy transfer processes are from these high-energy pigments physically distant from the reaction center to lower energy pigments that are physically closer to the reaction center (**Figure 3**). With each transfer, a small amount of energy is lost as heat, and the excitation is moved closer to the reaction center, where the energy is stored by photochemistry. Note, that the probability of excitation energy escapes from the trap in the form of fluorescence at all transfer steps is nonzero and depends on the intensity and wavelength of the excitation light.

During the energy transfer process, the occasional quenching of the absorbed light by fluorescence can occur and this becomes the essential property for fluorescent spectroscopy. It usually represents a small fraction of the excited states and diminishes in a functioning photosynthetic complex. Nevertheless, the fluorescence is an extremely informative quantity, because it reports on the energy transfer and trapping. Both steadystate and time-resolved fluorescence measurements are widely used methods for probing the organization and functional state of photosynthetic systems.

The unique spectroscopic properties of different cyanobacterial strains may become a promising fingerprints for practical and laboratory application [28]. The polypeptide composition of PBS varies widely among strains of cyanobacteria. However, it should be noted that the degree of PBS compositional variability, which reflects the ability of an organism to adapt to environmental changes, varies from strain to strain. Moreover, for a single strain, it also depends upon the environmental conditions such as nutrient availability, temperature, light quality, and light intensity.

The intact PBSs in cyanobacteria harvest sun light in the visible range from 400 to 750 nm and transfer the energy to the chlorophyll a (Chl a) of the photosystems PSII and PSI [24, 34, 35, 39]. When the single pigment-protein complexes aggregate in PBSs, their absorption bands are broadened due to the additional splitting of energy levels in the cause of interaction with other biliproteins and linker polypeptides. This leads to a more efficient harvesting of the light energy. Blue and red wavelengths of the visible light (around 440 and 675 nm) are mainly absorbed by cyclic tetrapyrroles, chlorophylls, combined in PSI and PSII, while green, yellow, and orange wavelengths (between 550 and 650 nm) are mostly absorbed by open-chained tetrapyrrole pigments, the phycobilins, composed in extramembranous antenna structures [24].

The fluorescence of intact living cyanobacterial cells is originated from the efficiency of the energy transfer between all components of the energy transfer chain including the final step, the delivery to PSII or PSI (**Figure 3(a)**). Each transfer step results in the spectrum shape as a peak or shoulder (**Figure 3(b)**). This is due to the fact that when phycobilisomes are bound to the thylakoid membrane, most of the energy from the last component of phycobilisome is channeled to chlorophylls in the thylakoid membrane and thus did not shade the fluorescence of the previous steps in energy transfer chain. In the course of the energy transfer from the initially photoexcited phycobiliprotein to the reaction center of photosystems PSI and PSII, fluorescence is emitted from almost every type of pigment and can be used as a probe to examine the mechanism of energy transfer within the light-harvesting system [8, 25, 26, 28].

A convenient way to monitor this energy transfer process is to irradiate a sample with light that is selectively absorbed by one set of pigments and then monitor fluorescence that originates from a different set of pigments. Obviously, if the energy transfer is taken place between pigments, the light absorbed by one set of pigments is emitted by another set differently depending on the excitation wavelength. This type of fluorescence excitation experiment can also be used to

measure quantitatively the efficiency of energy transfer from one set of pigments to another [26]. Moreover, different species of cyanobacteria contain different accessory pigment-proteins and specific linker-proteins between them, therefore a set of fluorescence emission spectra excited by different wavelengths have its own unique shape for the cells of one strain and are quite distinguishable from other species and strains. Such sets of fluorescence emission spectra can be used for automatic differentiation of cyanobacterial species.

3. Confocal laser scanning microscopy (CLSM)

CLSM applications in biology and medicine predominantly employ fluorescence. Cellular structures can be specifically labeled with dyes (fluorescent dyes = fluorochromes or fluorophores) in various ways. But the cyanobacterial photosynthetic pigments, chlorophyll a and phycobilins, have an inherent fluorescence at 543 and 633 nm excitation and 590–800 nm emission and need no labelling for visualization. To target other specific elements, many fluorescent dyes and labels can be used. In this study, we use CdSe/ZnS quantum dots for imaging extracellular substances. It is also possible to use the transmission mode with conventional contrasting methods, such as differential interference contrast (DIC), as well as to overlay the transmission and confocal fluorescence images of the same specimen area.

In the present investigation, both Leica TCS-SP5 and Carl Zeiss LSM 750 were used for investigation of living cyanobacterial cells. For Leica TCS-SP5, laser power settings are as follows: 29% of Ar laser power was reflected onto sample with Acousto-Optical Tunable Filter (AOTF) and further power percentage for its laser lines was: 30% of 458 nm laser-line and 10% for all other lines. A 405-nm line of diode UV laser was reflected onto sample with 3%, and HeNe laser lines 543 and 633 nm were reflected with 10% and 2%, respectively. An acousto-optical beam splitter (AOBS) was used to transmit sample fluorescence to detector.

For 2D imaging, Leica TCS-SP5 was utilized. To rise the sensitivity and contrast of 2D images, they were recorded at 405 nm excitation wavelength (diode UV laser) and by Leica HyD hybrid detector, which strongly improves contrast in comparison to PMTs. HyD gain: 100%. The images of 1024 × 1024 and 2048 × 2048 pixels were collected with a 63× glycerol immersion lens (glycerol 80% H_2O) with a numeric aperture of 1.3 (objective HCX PL APO 63.0 × 1.30 GLYC 37°C UV) and with additional digital zoom factor 10–35. The fluorescence emission images were accompanied with the transmission images (in the parallel channel), collected by a transmission detector with the photomultiplier voltages ranged from 300 to 500 V. The images were recorded with a pinhole setting of 1 Airy unit (the inner light circle of the diffraction pattern of a point light source, corresponds to a diameter of 102.9 μm with the lens used (see [1])).

Carl Zeiss LSM 750 with LSM Software ZEN 2009 was used for 3D-imaging. The images were collected with EC Plan-Neofluar 100×/1.3 oil M27 and with additional digital zoom factor 2.86. XY-scan of 1024 × 1024 pixel images was performed with resolution 8-bit in two channels. One pixel corresponds to 29.7 × 29.7 μm. A multi-dimensional acquisition tool was used for recording z-stack of 80 sections with z-step 0.10 μm.

Fluorescence emission spectra of the intact cells were measured by Leica TCS-SP5 at 8 excitation wavelengths corresponding to all available laser lines. The excitation wavelengths are: 458, 476, 488, 496, 514 nm—the lines of Ar laser, 405 nm is the line of diode UV laser and 543, 633 nm are the lines of HeNe laser. Chlorophyll fluorescence was excited by the 405, 458, 476, and 488 nm laser lines, and phycobilisome (PBS) fluorescence was induced by the 496, 514, 543, and 633 nm laser lines. Fluorescence emission was detected for PE at 570–600 nm, for

PC and APC at 650–670 nm, and for Chl a of both photosystems at 675–720 nm. The whole emission spectrum between 520 and 785 nm was recorded using the lambda scan function of the "Leica Confocal Software" by sequentially acquiring a series ("stack") of 38–45 images, each with a 6-nm fluorescence detection bandwidth and with 6-nm wavelength step. For obtaining fluorescence-intensity information, images of 512 × 512 pixels were collected with objective HCX PL APO 63.0 × 1.30 GLYC 37°C UV and with additional digital zoom factor 5–9. One pixel corresponds to 53.5 × 53.5 nm. The photomultiplier (PMT) voltages were used in the range from 900 to 1100 V. For better signal yield, lambda scans were performed with "low speed" setting (400 Hz) in bidirectional scan mode and with a pinhole setting of 1 Airy unit. Regions of interest (ROIs) representing single cells or subcellular regions were used to calculate fluorescence spectra.

In CLSM applications, the laser light density in the focus point is high. Dwell time and the intervals between the illuminations may influence photo-damage and saturation of photosynthesis. Thus, since most chromophores and natural pigments bleach under the high laser excitation energies, a bleach-test should be performed [40]. During the detection, the fluorescence of the main accessory pigments for each cyanobacterial strain should be controlled and the changes in their fluorescence should not exceed 10–20%. The power of individual laser lines should be chosen according to the photodamage they cause. In our experiments, the repeated spectra were obtained under selected excitation power at a fixed point in a cell to check whether the excitation would affect the cells. In each case, it was shown that at the chosen excitation energies, the fluorescence spectra did not vary within the experimental error during 10–15 records. When excitation energy was increased, both the height and the center of the fluorescent peaks varied enormously with time because of photodamage or structure-breakdown in photosynthetic systems.

In the experiments, where several laser lines were involved for the investigation, the first spectrum was recorded again at the end of each series to control the initial state of the cell. To visualize differences between strains with higher spectral and spatial resolution, lambda scans were performed with 6-nm bandwidth and with 6-nm steps. As far as the fluorescence intensities depend on the excitation energy (which varies for different laser lines), sensitivity setting of the photomultiplier, and the distance from the sample, all spectra were usually normalized to their maximum, and only qualitative analysis was performed.

3.1 Spectral imaging and spectral unmixing

In a conventional light microscope, object-to image transformation takes place simultaneously and parallel for all object points. The specimen in CLSM is irradiated in a pointwise fashion, that is, serially, and the physical interaction between the laser light and the specimen fluorescence is measured point by point. To obtain information about the entire specimen, it is necessary to guide the laser beam across the specimen. Line-by-line scanning of the specimen is carried out with a focused laser beam deflected in the X and Y directions by means of two galvanometric scanners, and pixel-by-pixel detection of the fluorescence emitted by the scanned specimen details is performed by photomultiplier tube (PMT) or by more sensitive hybrid detector (HyD).

For examining flat specimens such as cell culture monolayers, it is usually sufficient to acquire one XY image to obtain the desired information. The same applies if the specimen is a three-dimensional tissue section of which a single optical section is representative. The thickness of the optical section (slice) and the focal position are selected so that the structures of interest are contained in the slice. The lateral resolution of a 2D image is defined by the pixel size in X and Y. The pixel

size, in turn, varies with the objective used, the number of pixels per scan field, and the zoom factor. Pixels that are too large degrade resolution, whereas pixels too small require longer scanning times and thus bleach the specimen. The optimum pixel size for a given objective and a given zoom factor should be obtained for each special sample/experiment.

In this section, we examined changes in pigments of live, unfixed cells using spectral imaging. This technique captures an entire emission spectrum from every cell. The images corresponding to the four photosynthetic pigments have been pseudocolored for visualization purposes. The pseudocoloring is based on the colors shown in **Figure 5**: Chl a is red, PC-APC is green, and PE is light blue.

In **Figure 4**, images illustrated differences in fluorescence between diverse physiological states of Microcystis CALU 398 cells are presented. Two channels for fluorescence detection and one transmission channel were used. Channel 1 (a), colored false green, represents averaged fluorescence of PC and APC in the range 650–660 nm, channel 2 (b), colored false red, shows Chl a fluorescence at 678–710 nm, channel 3 (c) is a transmission microphoto, and in (d) all three channels are superimposed. Here small signal in both fluorescent channels corresponds to healthy cells, cells in bad physiological state (dying cells) have a high PC-fluorescence (green arrows), and dead cells have no fluorescence (white arrows). The high intensity in the shorter wavelength interval reflects that fluorescence in dying cells mainly originates from phycobilisomes at ca 650–660 nm. Healthy cells displayed weaker emission intensity over the whole spectral range, located at the periphery of the cells. This response correlates with effective light utilization and energy balance [26].

Figure 5 represents confocal laser scanning photomicrographs illustrating photosynthetic pigment localization in filamentous cyanobacterium Phormidium CALU 624. False color overlay images were obtained by simultaneous three channel

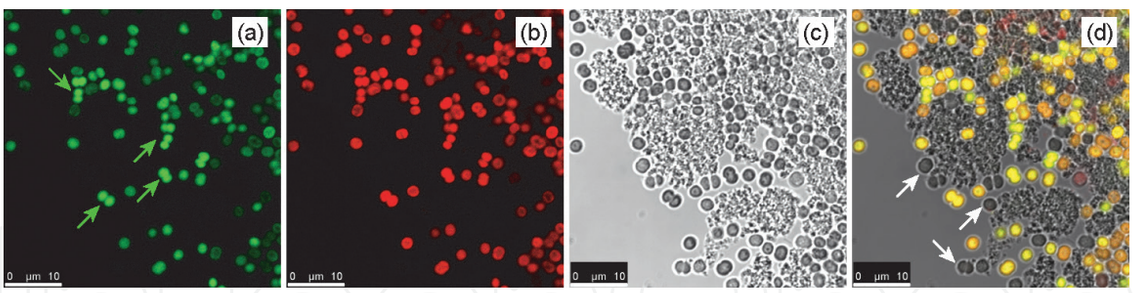

Figure 4.
CLSM micrographs of cyanobacterium Synechocystis 1336, visualized with CLSM. Green channel (a) represents fluorescence from phycobilins at 656 nm, red channel (b) from chlorophyll a at 682 nm, (c) represents transmission image and an overlap of all three is shown in (d). Scale bar = 10 µm.

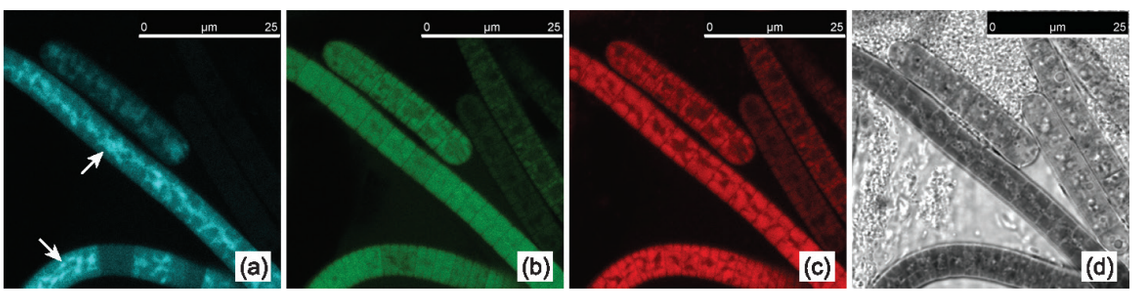

Figure 5.
False color overlay images of Phormidium CALU 624 cells at stationary phase of growth are visualized by CLSM simultaneously in three fluorescence detection channels. (a) Channel 1 (light blue): fluorescence signal from PE (575–585 nm), (b) channel 2 (green): PC-APC (650–660 nm), (c) channel 3 (red): Chl a (678–710 nm), and (d) channel 4: transmission microphoto. Scale bar = 25 µm.

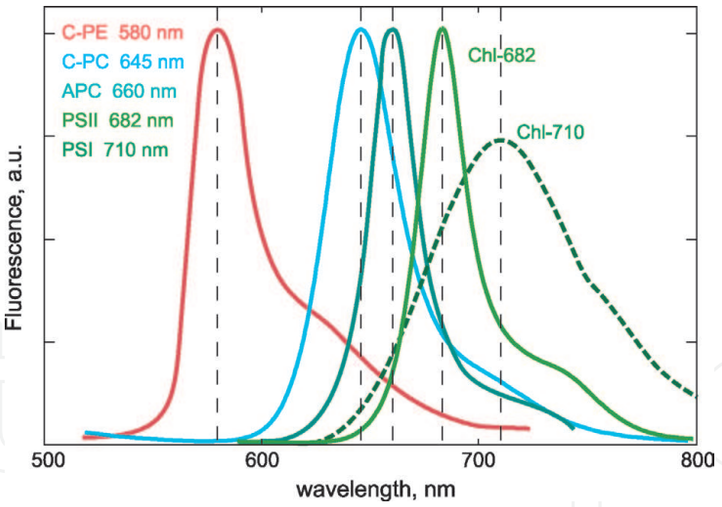

Figure 6.
Fluorescence spectra of individual phycobiliproteins, which can be used as reference data for spectral unmixing. Spectra were normalized to their maximum, and all values were adapted to our measurement conditions. The dashed lines indicate the respective fluorescence maxima (PE—580 nm; PC—645 nm; APC—660 nm; Chl (PSII)—682 nm; Chl (PSII)—710 nm).

fluorescence detection. Fluorescence images (**Figure 5(a)–(c)**) were obtained at different emission wavelengths, excited by a 405 nm laser beam. The fluorescence signal was collected at 647–652, 658–663, and 675–680 nm, and the false colors light blue, green, and red in **Figure 5(a)–(c)** represent the fluorescence emitted by PE, PC-APC, and Chl a, respectively. The highest intensity signal of PE-fluorescence is located in the center of the cells (white arrows), and the strongest signal from Chl a fluorescence is located at the cell periphery, the latter provides the evidence of the thylakoid arrangement.

Fluorescence spectra of living cyanobacterial cells are composed of overlapping fluorescence emission spectra from several photosynthetic pigments. The application of spectral unmixing with reference spectra for individual pigments (**Figure 6**) can give more pronounced and detailed images of pigment localization. Spectral unmixing can also be used to calculate the relative fluorescence shares of the individual pigments contributing to the spectrum.

Spectral unmixing is a method for the complete separation (unmixing) images with overlapping emission spectra. It is used with specimens labeled with more than one fluorescent dye, exhibiting excitation and emission crosstalk or with self-fluorescent specimens contained of several photosynthetic pigments (as in our case).

If we regard a pixel of a lambda stack that represents a locus in the specimen where several fluorescent pigments with their known reference spectra overlap, the cumulative measured spectrum can be expressed as a linear combination of the reference spectra multiplied by the corresponding intensity for each pigment. By means of known reference spectra, this equation can be solved for the intensities of each pigment. The reference spectra can either be loaded from a spectra database, or from literature [40–44], or directly extracted from the lambda stack. Obtained linear unmixing function will generate a multi-channel image, in which each channel represents only one pigment. The accuracy of the technique allows the complete unmixing even of such dyes or self-fluorescence pigments whose spectra have almost identical emission maxima.

Unfortunately, in living cyanobacterial cells, it meets some difficulties. The problems are caused by the fact that the light absorption and emission properties of isolated phycobiliproteins are rather different from those of the intact phycobilisomes in the living cyanobacterial cells. In living cells, the spectral properties

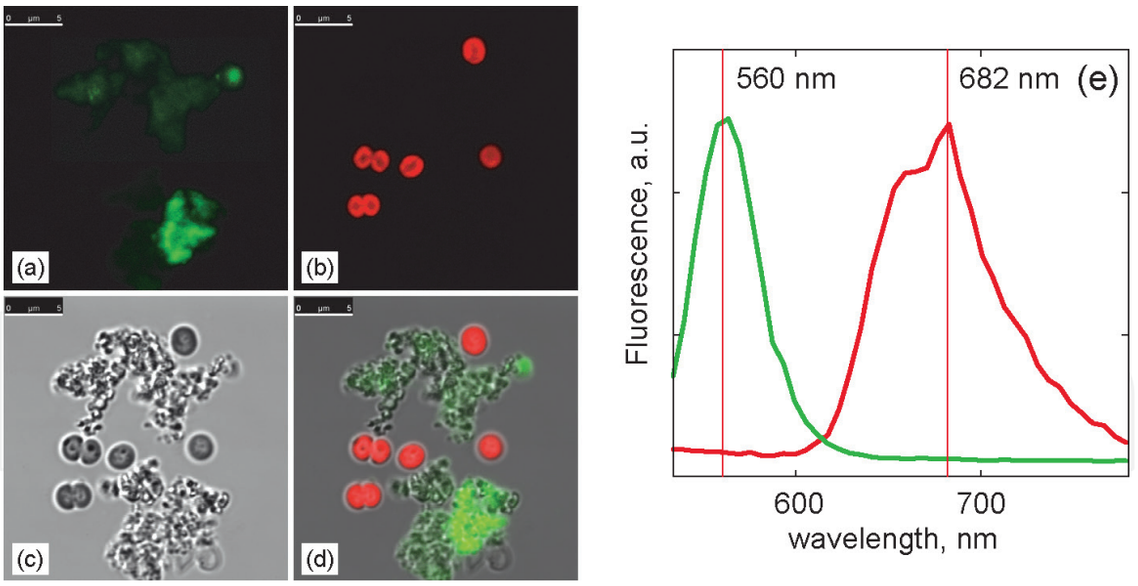

Figure 7.
Simultaneous observation of self-fluorescent photosynthetic cells of Microcystis CALU 398 and labeled by quantum dots extracellular polysaccharide. (a) Channel 1: quantum dots fluorescence (green), (b) channel 2: natural pigment fluorescence (red), (d) channel 3: corresponding transmission image, (d) all three channels superimposed. Fluorescence spectra in (e) have the colors corresponding to (a) and (b). Scale bar = 5 μm.

of pigments from certain organisms may differ crucially from the properties of the dissolved ones, for example, spectra of the components can vary in peak widths and may be shifted in wavelength due to the different pigment-protein and linker connections. In this case, only hyperspectral CLSM measurements [42] can give suitable reference spectra for decomposition.

If the overlapping of the emission spectra of the fluorescent components is not very much, then the image spectral unmixing can be easily obtained without any calculations. The example of such unmixing is presented in **Figure 7**. In **Figure 7**, the usage of combination of natural pigment fluorescence and fluorescence probes for imaging of cyanobacteria and their extracellular polymeric substances (polysaccharides) is demonstrated. To target extracellular substances, fluorescent labels should be used. Here, nonfluorescent polysaccharides were labeled by quantum dots CdSe/ZnS. Quantum dots have a fluorescence in green (520–580 nm) when excited by ultraviolet light (405 nm) and photosynthetic pigments of Microcystis CALU 398 have a fluorescence in red (620–780 nm). Thus the fluorescent signals will not overlap. The reference spectra for quantum dots and Microcystis CALU 398 cells were obtained by means of lambda scanning (**Figure 7(e)**).

3.2 3D bio-imaging

In addition to the possibility to observe a single plane (or slice) of a thick specimen in good contrast, optical sectioning allows a great number of slices to be cut and recorded at different planes of the specimen, with the specimen being moved along the optical axis (Z) by controlled increments. The result is a 3D data set, which provides information about the spatial structure of the object. The quality and accuracy of this information depend on the thickness of the slice and on the spacing between successive slices.

Once a 3D stack of images has been recorded, the user has various presentation options. The data may be displayed as a gallery of depth-coded images or as orthogonal projections of the XY, XZ, and YZ planes. To create a 3D impression on a 2D monitor, animations of different viewing angles versus time, 3D reconstruction, shadow projections, and surface rendering techniques are possible.

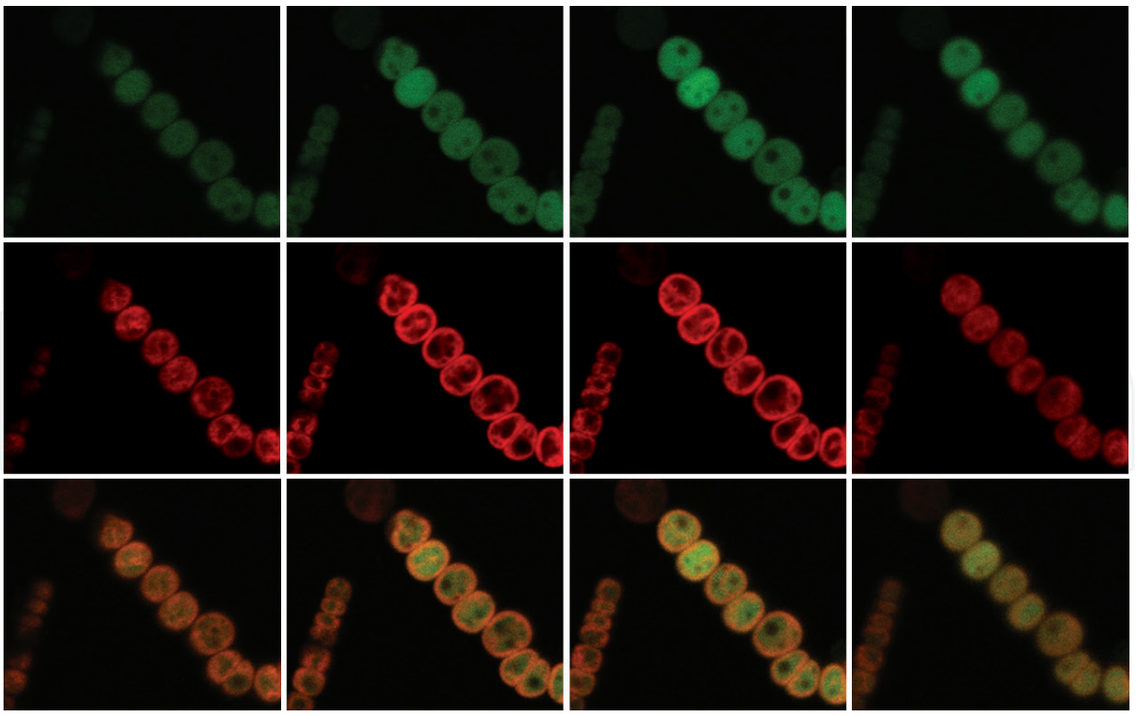

Figure 8.
Pigment localization through the depth. Two-dimensional sections of Anabaena CALU 824. Green channel: PE-fluorescence, red channel: Chl a-fluorescence, and bottom panel: two channels superimposed.

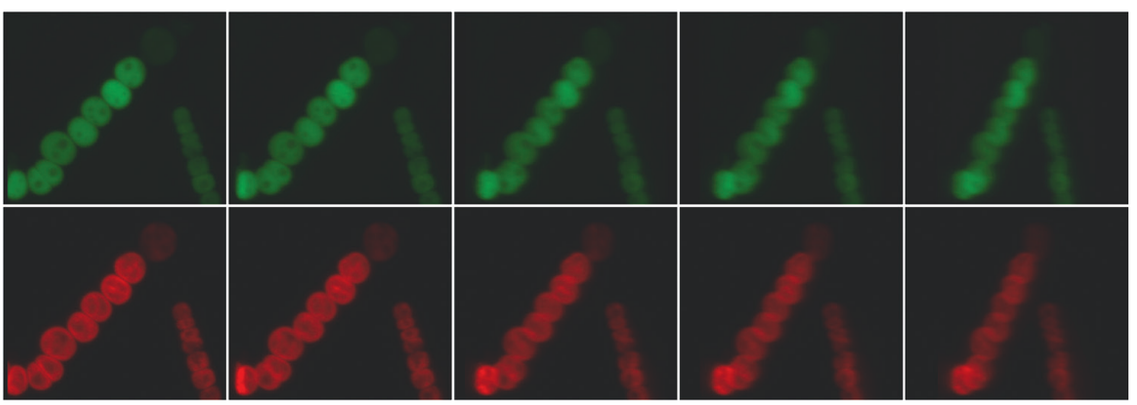

Figure 9.
Several frames from animation of 3D-model at different viewing angles. Two colors correspond to two fluorescent channels: green channel—PE-fluorescence and red channel—Chl a-fluorescence.

In **Figure 8**, several two-dimensional optical sections of a filament of Anabaena CALU 824, obtained by Carl Zeiss LSM 710 with LSM Software ZEN 2009, are shown. A series of XY images (z-stack), acquired in different focus positions represents the Z dimension of the specimen. Here we present images from two channels: green—PE-fluorescence, red—Chl a-fluorescence, and the bottom panel—two channels superimposed. To calculate 3D model from z-stack, much more sections should be acquired.

Figure 9 shows several frames from 3D reconstruction animation computed from a 3D data set in ImageJ 1.46r software (http://imagej.net/). To render 3D-model z-stack containing 80 images were recorded with 0.1 μm increment along z-axis.

3.3 Single-cell spectroscopy (lambda scanning)

Fluorescence spectra of living photosynthetic cells can be reliably analyzed by a microspectrofluorometric method (CLSM spectroscopy), which is implemented

in many modern CLSMs. This method allows the precise localization of the fluorescence signal, even within a single living cell. Modern fluorescence microscopic spectroscopy or confocal laser scanning microscopic spectroscopy provides a unique opportunity to obtain the intrinsic fluorescence emission spectra from cyanobacterial cells in vivo [40–43, 45–46]. Moreover, using spectral unmixing, the fluorescence of individual spectral components can be resolved, and their relative intensities can be calculated [1–2].

The acquisition of spectral data becomes necessary when the cellular parameter to be measured is coded by changes of the emission spectrum. PMT element registers sequentially a different part of the spectrum, each part having a spectral width of 6 nm with a step 6 nm. The result is a lambda stack of XY images in which each image represents a different spectral window. Lambda stack is a series of images showing the same area, but in different spectral windows. From a lambda stack, the intensity of the signal for each pixel of the image can be extracted as a function of wavelength. These spectral "fingerprints" can easily be obtained for any image area by means of the mean of ROI function.

Although, the pigment structure of different cyanobacterial strains has been intensively investigated, the variations in self-fluorescent spectra of single cells for different cyanobacterial species has not been analyzed yet. We suppose that the best way to investigate the in vivo operation of photosynthetic system is a single-cell fluorescence microscopic spectroscopy. Single-cell detection can provide the information on small peculiarities that is regularly buried in normal ensemble average experiments. This is thus a good way to study the time evolution process and spectroscopic properties of individual cells. Both steady-state and time-resolved fluorescence measurements can be used for probing the intrinsic self-fluorescence by means of CLSM.

As it was mentioned above, phycobilisomes contains several kinds of biliproteins, and their fluorescence spectra reflect the contribution of each (**Figure 3**). Moreover, depending on the excitation wavelength, the room temperature fluorescence emission spectrum of intact cyanobacterial cells exhibits various extents of contribution of phycobilisome emission to the spectrum. If one exclusively excites Chl a, using a 458-nm line of an Ar laser, the emission spectrum by cyanobacterial cells shows no appreciable emission of PC or APC. This is indicated by PSI emission band at 715 nm and PSII emission band at 682 nm (**Figure 10**). The excitation by intermediate (blue and green) wavelengths (405, 488, and 496 nm) reveals fluorescent maxima of all photosynthetic pigments, as the light in this range is absorbed by all pigment-protein complexes almost in equal portions, and fluorescence emits by all steps of energy transfer chain (**Figure 3**). The direct excitation of cells in the PC absorption region at 514 and 543 nm results in emission spectrum with two main peaks at 580 and 656 nm, which are due to PE, PC, and APC emission. The spectra of the 633 nm excitation directly gives a prominent emission band at 656 nm, that originates from PC, omitting band at 580 nm, which cannot be excited by 633 nm, even for species that have PE. Other small emission bands, corresponding to fine pigment structure of antenna complex, are not resolved at room temperature. Comparative analysis of the series of fluorescence spectra for different cyanobacterial species and strains reveals visible variations in their shape (**Figure 10**). If the fluorescence spectra were taken from alive cells in normal physiological state, which are cultured in the same growth environmental conditions, then the interspecies variations in pigment/Chl a ratios are more pronounced than variations within the individual species. And species/strains differentiation could be carried out on the base of fluorescence analysis [3, 6–7].

Figure 10 shows the experimental sets of single-cell fluorescence spectra for Microcystis CALU 398, Merismopedia CALU 666, Leptolyngbya CALU 1715,

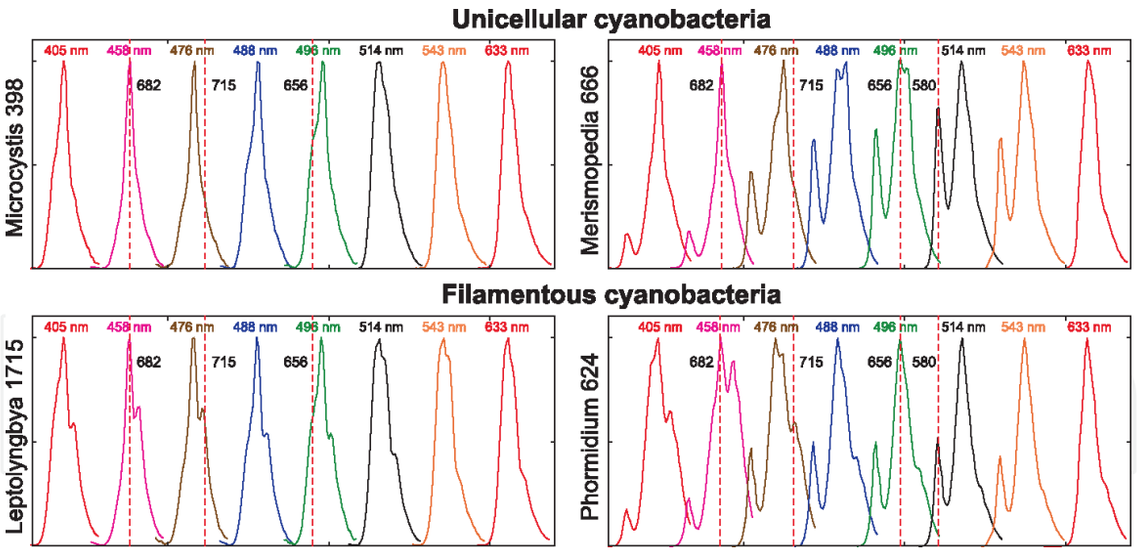

Figure 10.
Single-cell fluorescence spectra of different cyanobacterial strains (unicellular and filamentous): Microcystis 398, Merismopedia 666, Phormidium 624, and Leptolyngbya 1715. The excitation wavelengths (405, 458, 476, 488, 496, 514, 543, and 633 nm) are given over the curves. All spectra are normalized to the maximum intensity and shifted along X-axis for convenience of observation. The dashed lines indicate the fluorescence maxima of the individual pigments (PE—580 nm; PC—656 nm; Chl a—682, 715 nm).

and Phormidium CALU 624 (cyanobacterial strains are labeled according to CALU collection of the Core Facility Center "Centre for Culture Collection of Microorganisms" of the Science Park of St. Petersburg State University). Each spectrum set was obtained by means of confocal laser scanning microscope (CLSM) Leica TCS-SP5, using different laser-lines for excitation (405, 458, 476, 488, 496, 514, 543, and 633 nm). Corresponding excitation wavelengths are given over each spectrum. All spectra are normalized to the maximum intensity and shifted along X-axis for convenience of observation.

Fluorescence of photosynthetic pigments in the intact cells is affected by physicochemical and physiological processes that occur within and across the thylakoid membranes. The structure and function of the thylakoid membrane can alter under stress conditions. The alterations may be both short- and long-term, depending on the nature and duration of the stress. The dynamical changes in fluorescent spectra of living cyanobacterial cells in different stress states can be detected via time-resolved CLSM measurements and can be used for estimation of the physiological state and viability of cyanobacterial cultures at different experimental stages.

Figure 11 illustrates the temporal changes of in vivo fluorescence spectrum taking place in the living cell of cyanobacteria strain Synechocystis CALU 1336 under high-light and heat stress. The excitation wavelength in this experiment was 488 nm. The set of spectra was obtained from a single cell during 45 min with 1 min step under over-excitation conditions (only every fourth spectra is presented in **Figure 11(a)**). At first, several minutes (1–12 min) spectrum changes slightly and mostly in the range of PC-fluorescence (around 656 nm). Since 488 nm light is absorbed primarily by PC and Chl a, photosynthesis and energy transfer chain are quickly saturated and reaction centres closes, thus the fluorescence around 656 nm starts growing. During the next few minutes (12-28 min) a rapid growth of PC-APC fluorescence indicates that over-excitation leads to the uncoupling of phycobilisomes from thylakoid membrane, while the Chl a fluorescence remains almost the same during this time period (see **Figure 11(b)**). Small rise of the Chl a fluorescence intensity at 20–39 min can be explained by strong overlapping of Chl a and PC-APC emission spectra, which leads to a crosstalk between these fluorescent signals. Then, after 30 min of irradiation, the degradation of detached phycobilisomes and PSII

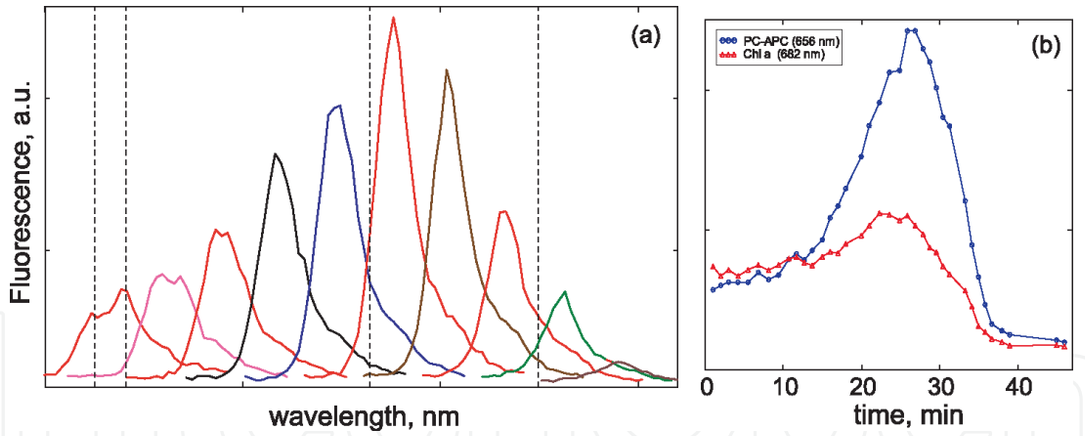

Figure 11.
Time degradation of living cell of cyanobacterial strain Synechocystis CALU 1336 under high-light and heat stress. (a) Spectra recorded at the excitation wavelength 488 nm with the time-step 4 min. All spectra are shifted along x-axis for convenience of observation. (b) Time dependence of the fluorescence intensity at 656 nm (PC-APC fluorescence) and at 682 nm (Chl a fluorescence).

pigment-protein complexes begins. The intensity of Chl a and PC-APC fluorescence decreases, and maximum is shifted to shorter wavelengths.

Two presented examples of CLSM lambda-scan application show the unique abilities of CLSM microscopic spectroscopy for investigation of physiological processes in cyanobacterial cells. More examples can be found in [3–5, 47].

3.4 Using fluorescence recovery after photobleaching (FRAP)

A field of growing importance is the investigation of living specimens that show dynamic changes. Dynamic processes in living specimens can be recorded by means of time series implemented in modern CLSMs. Data once acquired can be analyzed "off-line," that is, after image acquisition. Time series are defined by a start time and the time interval between two successive images. To analyze a time series, some option allows fluorescence intensity changes to be quantified in defined regions of interest (ROIs).

Within a time series, the CLSM permits selective, point-accurate illumination of ROIs with laser light. This function is useful for generating a photobleaching routine, for example, within a FRAP experiment (fluorescence recovery after photobleaching), for analyzing dynamic processes. Complex time series experiments, with different images to be taken at different sites within a specimen according to a defined time pattern, can be carried out by means of CLSM software.

Fluorescence recovery after photobleaching (FRAP) is a technique widely used in cell biology to observe the dynamics of biological systems. In photosynthetic organisms, it can be directly used, for example, for investigation of the dynamics of thylakoid membranes, including the diffusion of membrane components [39, 48–52].

Diffusion of membrane components is involved in a number of processes, for example, in investigation if the chromatic adaptation of light-harvesting apparatus, in describing of the electron transport in photosynthetic membranes and in studies of the biogenesis, turnover, and repair of the photosystems. Diffusion coefficients for certain thylakoid membrane components can also be estimated by indirect methods [53, 54], but FRAP and related optical techniques may be used for direct observation of the diffusion in biological systems.

The component whose diffusion is to be observed must be bleached by high laser power with the confocal spot scanning briefly over a small area of the sample. After bleaching, the laser power is decreased, and the whole sample is imaged. The bleached area of the sample will be seen as a dark, nonfluorescent patch on the image. Then the sample is repeatedly imaged, and if the bleaching will change

somehow during the time, the diffusion coefficient can be derived from these characteristic changes [48, 49]. Usually the component whose diffusion is to be observed must be tagged with a fluorophore, but, as it was mentioned above, the great advantage of photosynthetic membranes is that their protein complexes are naturally fluorescent, so their diffusion can be observed without any necessity for specific fluorophore binding or GFP gene fusions. The only requirements for quantitative FRAP are that the membrane geometry is known, and the membrane environment is uniform over an area considerably larger than the area of the bleach. Unfortunately, most green plant thylakoid membranes have an intricate, convoluted structure, and extensive lateral heterogeneity on small scales. On the other hand, some cyanobacterial species have the membrane systems located in the periphery of the cell and are uniform enough in small regions. Anyway, by means of FRAP technique, it is always possible to see if particular components are mobile or not, to make a rough estimation of time-scales and to investigate a number of factors that affect their diffusion coefficient.

In contrast to typical green plants, in most cyanobacterial strains, there is no thylakoid membrane stacking and no extensive lateral heterogeneity. The preferred model organism used in previously published papers [39, 48, 49] is the cyanobacterium Synechococcus sp. PCC7942, which has suitable membrane conformation and is also well-characterized and transformable. Its cells can be elongated up to 10–20 μm by means of some growth techniques to achieve lateral heterogeneity in relatively large region. But in this work, we demonstrate that reasonable results can be obtained even for spherical cells of Microcystis firma CALU 398.

It is well known that phycobilisomes diffuse rapidly on the surface of the thylakoid membrane, while PS II reaction centers are normally almost immobile. Here we used FRAP to measure the mobility of phycobilisomes in the intact cyanobacterial cells. These experiments indicate that phycobilisomes may frequently decouple from reaction centers and diffuse randomly before attaching to another reaction center.

FRAP measurements were carried out with a laser-scanning confocal microscope Leica TCS-SP5. During the measurement, a series of images of the cell is recorded, and it is important to keep the laser power low enough not to cause significant further bleaching of the cell during repeated imaging. The basic procedure for the measurement is to record an image of the sample cell before bleaching (**Figure 12(a)**(1). Then the laser power is increased by a factor of 8–10, and the confocal spot is scanned only over a restricted area of the sample (light-blue vertical rectangle) to bleach out most of the fluorescence in that area. The laser power is then reduced again, and a series of post-bleach images is recorded. The best time-scale for the measurement depends on the rate of diffusion and has to be found by trial and error. In thylakoid membranes, the diffusion of both lipids and proteins is generally rather slow and a 1 s bleach, followed by a series of images recorded at 1.3 s intervals, was adequate to capture diffusion.

Figure 12 summarizes the steps involved in recording and analyzing FRAP data. In the presented experiment, a one-dimensional diffusion of phycobilisomes was measured in a cell of the cyanobacterium Microcystis firma CALU 398. Confocal laser scanning microscope Leica TCS-SP5 with immersion objective HCX PL APO 63.0x1.30 GLYC 37°C UV was utilized in this investigation. The He-Ne laser (633 nm, 150 mW) was used for excitation in both bleaching and scanning modes, and the laser power was 25 and 2% correspondingly. The vertical (Z) resolution was 0.2 μm, and the resolution in the x-y plane was about 24.1 nm. Digital zoom was 20. The laser was scanned over the sample with oscillating mirrors. Scan speed was 400 Hz. Fluorescence from the sample was separated from the excitation light with a beam-splitter, passed through a 102.9 μm pinhole and detected with a photomultiplier with PMT voltage 1000 V. The emission band for recorded images was 673–678 nm.

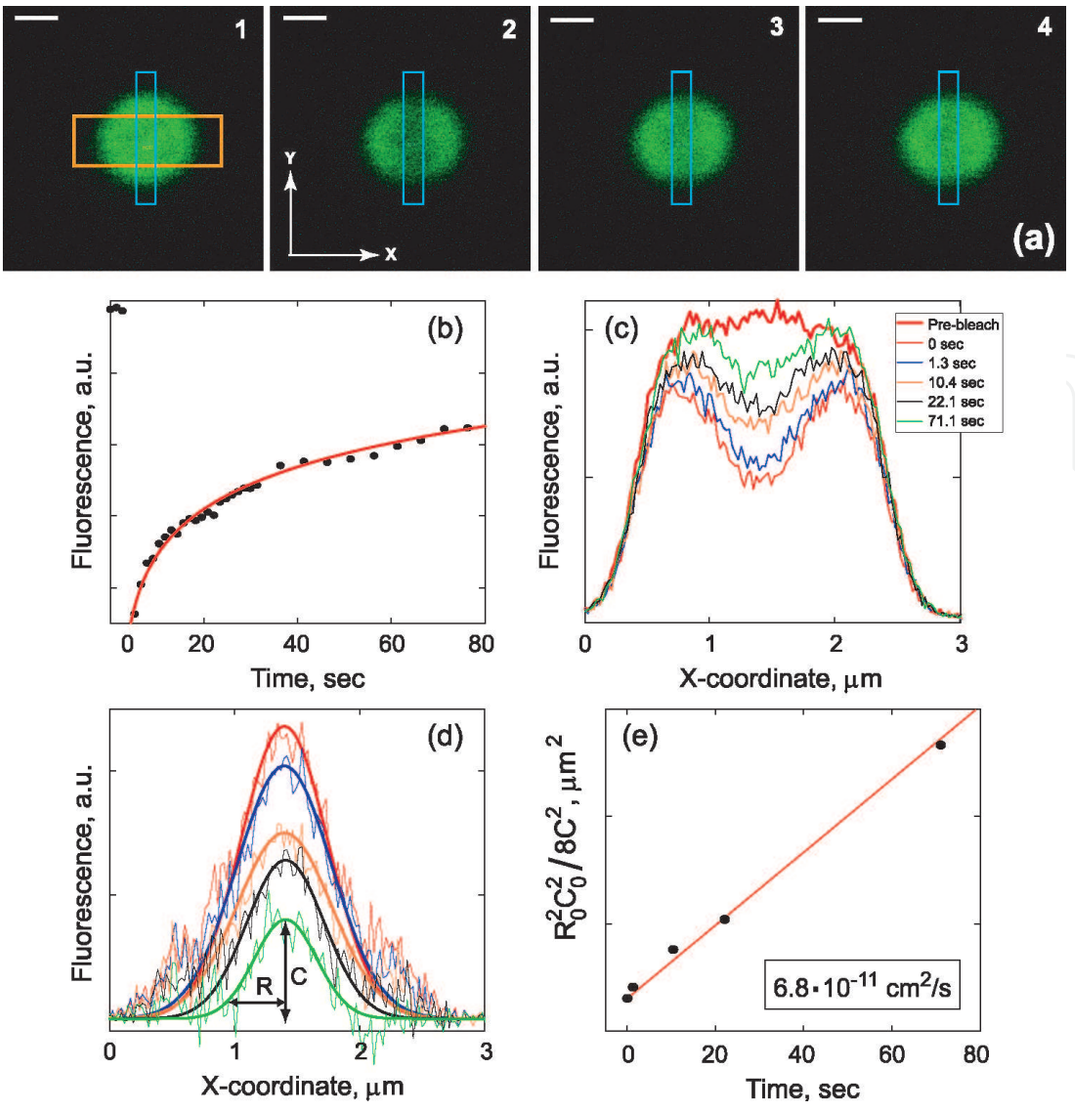

Figure 12.
Extracting data from a FRAP experiment on a cell of Microcystis CALU 398. (a) Fluorescence intensity images from FRAP-sequence, taken at −5, 0, 10.4, and 71.1 s, correspondingly. ROI 1 (light blue rectangular): bleaching area and ROI 2 (orange rectangular): the area for controlling fluorescence intensity profile across bleaching region. Scale bar = 1 μm. (b) Total fluorescence intensity of bleached area as a function of time. The recovery of the fluorescence is presented as open circles and exponential fitting function—solid line. (c) Pre-bleach and post-bleach fluorescence intensity profiles across bleaching region at t = 0, 1.3, 10.4, 22.1, and 71.1 s. (d) The subtracted post-bleach and pre-bleach fluorescence intensity profiles and corresponding Gaussian fitting curves at five time-points indicated at (c). (d) A plot of C-function for one-dimensional diffusion versus time. The obtained diffusion coefficient is indicated on the plot.

The first image (**Figure 12(a)**(1) was recorded prior to bleaching, by scanning the confocal spot in the XY mode. Excitation wavelength was at 633 nm, and the detection range was from 650 to 750 nm. The scan was then switched to another mode, the laser power was increased by a factor of 12, and the sample was bleached by scanning the laser repeatedly in one dimension across the cell for 1 s. Light-blue vertical rectangle indicates bleaching area. Then the laser power was reduced again to the initial value, the scan was switched back to the XY mode, and the cell was imaged by scanning over a square of 12.30 × 12.30 μm in the x-y plane (512 × 512 pixels) (**Figure 12(a)**(2–3). There was no detectable photobleaching during the recording of successive image scans. A series of 20 further images were recorded at time intervals 1.3 s and then another 10 images at time intervals 5 s. Images (a3) and (a4) show the state at 20th and 30th point (10.2 and 71.1 s, correspondingly). Within a few minutes, the bleaching profile spreads, becoming broader and shallower. This shows that phycobilisomes are diffusing, with unbleached phycobilisomes diffusing into the bleached area.

Leica software (LAS AF Lite 2.6) was used to extract the fluorescence profiles across the bleaching area (orange rectangle) from the images, summing all the pixel values in the Y-direction for each X coordinate. And then MathCad 14 was used for curve fitting and further calculations.

(**Figure 12(b)**) shows a typical time dependence of fluorescence recovery after photobleaching. The open circles denote the integrated signals over the bleached area, marked by the light-blue vertical rectangle in the fluorescence intensity images (a), and the line represents a fitting curve. First three points correspond to pre-bleaching images. Then goes a 1-s gap corresponds to bleaching period. The next 20 points were recorded with step 1.3 s and another 10 points with step 5 s.

One pre-bleach and five post-bleach fluorescence profiles across the bleaching area (orange rectangle) at a series of time-points were aligned (**Figure 12(c)**). The post-bleach profiles (shown in thin lines) were corrected by subtracting the pre-bleach profile (shown in thick red line), and the Gaussian curves were then fitted to the corrected fluorescence profiles (**Figure 12(d)**). The fitted Gaussian curves were used to obtain corresponding depth (C) and the half-width (1/e2) (R) of the bleach. Note that the bleaching profile remains Gaussian, but becomes broader and shallower with time. The change in C and R with time and diffusion distance in one dimensional diffusion model can be described according to the equation given in [49]. Finally, a suitable function of C is plotted versus time in (**Figure 12(e)**) and the corresponding diffusion coefficient was obtained. Here, R0 and C0 are the values of R and C at time just after bleaching. For one-dimensional diffusion, the plot shown in (**Figure 12(e)**) should be linear with gradient equal to the diffusion coefficient. The calculations for the diffusion coefficient of phycobilisomes give a result of 6.8 × 10–11 cm^2/s, which is similar to those given in [49]. Together with the linearity of the plot in **Figure 12(e)**, this indicates that this procedure can be applied to spherical cells also and that our measurement does not greatly perturb the system.

4. Conclusion

Light microscopy has been used for studying cells for many years and has advanced our understanding of key cellular processes. However, fixation involves nonphysiological procedures and only provides a snapshot view of cells at a single point in time. To truly understand cellular function, we need to extend our imaging capabilities in ways that enable us to follow sequential events in real time, monitor the kinetics of dynamic processes, and record sensitive or transient events. And CLSM gives such opportunity. In addition, CLSM technique allows the investigation not only cultivable, but also the noncultivable phototrophic microorganisms.

This study presents simple and practical advices for performing special confocal microscopy applications. Our approach allows to study detailed mechanisms of photoprotection and stress reactions in different cyanobacterial species. Fluorescence spectra of cyanobacterial photosynthetic pigments are easily recorded by spectral CLSM. The fluorescence shares of individual phycobiliproteins can be reliably determined by spectral unmixing, showing that the spectral resolution of CLSM is well suited for this approach.

Finally, with the advent of live cell imaging and the development of high- and superresolution technologies, it is now possible to acquire data on viable cells in a biologically relevant context providing us with a greater insight of cellular function than has previously been possible.

Note here, that there are a lot of additional techniques already implemented in modern CLSMs, which open new perspectives for single-cell investigation, such as: white laser, which provides the ability to obtain not only fluorescence emission

spectra, but also single-cell excitation and absorption spectra [55]; hyperspectral CLSM which allows more precise fluorescence spectra through the cell thickness and gives more detailed fluorescent pigments location [42]; STED and multi-photonic techniques, that extend the CLSM abilities to single-molecular studies [56, 57]. They are the subject for further investigations.

Author details

Natalia Grigoryeva[1*] and Ludmila Chistyakova[2]

1 Saint-Petersburg Research Center for Ecological Safety, Russian Academy of Sciences, Saint-Petersburg, Russia

2 Saint-Petersburg State University, Saint-Petersburg, Russia

*Address all correspondence to: renes3@mail.ru

References

[1] Pawley JB, editor. Handbook of Biological Confocal Microscopy. Boston, MA: Springer; 1995. 346 p. DOI: 10.1007/978-1-4757-5348-6

[2] Wilson T. Confocal Microscopy. London: Academic Press; 1990. 426 p. DOI: 10.1007/978-1-4615-7133-9

[3] Grigoryeva N, Chistyakova L. Fluorescence microscopic spectroscopy for investigation and monitoring of biological diversity and physiological state of cyanobacterial cultures. In: Tiwari A, editor. Cyanobacteria. London: IntechOpen; 2018. pp. 11-44. DOI: 10.5772/intechopen.78044

[4] Rumyantsev VA, Grigor'eva NY, Chistyakova LV. Study of changes in the physiological state of cyanobacteria caused by weak ultrasonic treatment. Doklady Earth Sciences. 2017;**475**(2):939-941. DOI: 10.1134/S1028334X17080190

[5] Grigoryeva NY, Chistyakova LV, Liss AA. Spectroscopic techniques for estimation of physiological state of blue-green algae after weak external action. Oceanology. 2018;**58**(6):896-904. DOI: 10.1134/S0001437018060061

[6] Jhangirov TR, Perkov AS, Grigoryeva NY, Chistyakova LV, Liss AA. Application of linear discriminant analysis for classification of cyanobacteria by intrinsic fluorescence spectra. Izvestiya SPbGETU "LETI". 2018;**5**:45-55 (in Russian)

[7] Grigoryeva NY, Chistyakova LV, Liss AA, Klionskiy DM, Perkov AS, Zhangirov TR. Neural networks application for automation of environmental monitoring of cyanobacterial blooms in open water. In: Proceedings of XXI IEEE International Conference, Soft Computing and Measurements (SCM), 23-25 May 2018, Saint-Petersburg, Russia. Vol. 2. Saint-Petersburg: Izd. SPbGETU "LETI"; 2018. pp. 210-213 (in Russian) ISBN: 978-5-7629-2239-5

[8] Papageorgiou GC. Fluorescence emission from the photosynthetic apparatus. In: Eaton-Rye J, Tripathy B, Sharkey T, editors. Photosynthesis. Advances in Photosynthesis and Respiration. Vol. 34. Dordrecht: Springer; 2012. pp. 415-443. DOI: 10.1007/978-94-007-1579-0_18

[9] Yokono M, Takabayashi A, Akimoto S, Tanaka A. A megacomplex composed of both photosystem reaction centres in higher plants. Nature Communications. 2015;**6**:6675. DOI: 10.1038/ncomms7675

[10] Abed RM, Dobretsov S, Sudesh K. Applications of cyanobacteria in biotechnology. Journal of Applied Microbiology. 2009;**106**(1):1-12. DOI: 10.1111/j.1365-2672.2008.03918.x

[11] Vijayakumar S, Menakha M. Pharmaceutical applications of cyanobacteria–A review. Journal of Acute Medicine. 2015;**5**(1):15-23. DOI: 10.1016/j.jacme.2015.02.004

[12] Singh S, Kate BN, Banerjee UC. Bioactive compounds from cyanobacteria and microalgae: An overview. Critical Reviews in Biotechnology. 2005;**25**(3):73-95. DOI: 10.1080/07388550500248498

[13] Liu L. New bioactive secondary metabolites from cyanobacteria [thesis]. Helsinki: University of Helsinki; 2014

[14] Grewe CB, Pulz O. The biotechnology of cyanobacteria. In: Ecology of Cyanobacteria II. Netherlands: Springer; 2012. pp. 707-739. DOI: 10.1007/978-94-007-3855-3_26

[15] Rastogi RP, Sinha RP. Biotechnological and industrial significance of cyanobacterial secondary metabolites. Biotechnology Advances.

2009;**27**(4):521-539. DOI: 10.1016/j.biotechadv.2009.04.009

[16] Anahas AM, Muralitharan G. Characterization of heterocystous cyanobacterial strains for biodiesel production based on fatty acid content analysis and hydrocarbon production. Energy Conversion and Management. 2018;**157**:423-437. DOI: 10.1016/j.enconman.2017.12.012

[17] Lei Y, Chen W, Mulchandani A. Microbial biosensors. Analytica Chimica Acta. 2006;**568**(1-2):200-210. DOI: 10.1016/j.aca.2005.11.065

[18] Reshetilov AN. Biosensor development in Russia. Biotechnology Journal: Healthcare Nutrition Technology. 2007;**2**(7):849-862. DOI: 10.1002/biot.200700021

[19] Ignatov SG, Ferguson JA, Walt DR. A fiber-optic lactate sensor based on bacterial cytoplasmic membranes. Biosensors and Bioelectronics. 2001;**16**(1-2):109-113. DOI: 10.1016/S0956-5663(00)00144-5

[20] Gault PM, Marler HJ, editors. Handbook on Cyanobacteria: Biochemistry, Biotechnology and Applications, Bacteriology Research Developments Series. New York: Nova Science Publishers; 2009. 538 p. ISBN: 978-1-60741-092-8

[21] Whitton BA editor. Ecology of Cyanobacteria II: Their Diversity in Space and Time. Netherlands: Springer Science & Business Media; 2012. 760 p. ISBN: 978-9-40073-855-3

[22] Seckbach J, editor. Algae and Cyanobacteria in Extreme Environments. Israel: Springer Science & Business Media; 2007. 786 p. DOI: 10.1007/978-1-4020-6112-7

[23] Huisman J, Matthijs HC, Visser PM, editors. Harmful Cyanobacteria, Aquatic Ecology Series. Vol. 3. Dordrecht: Springer; 2005. 243 p. DOI: 10.1007/1-4020-3022-3

[24] Bryant DA, editor. The Molecular Biology of Cyanobacteria, Advances in Photosynthesis. Vol. 1. Dordrecht: Kluwer Academic Press; 1994. 881 p. DOI: 10.1007/978-94-011-0227-8

[25] Green BR, Parson WW, editors. Light-Harvesting Antennas in Photosynthesis, Advances in Photosynthesis and Respiration. Vol. 13. Dordrecht: Springer Netherlands Kluwer Academic Publishers; 2003. 514 p. DOI: 10.1007/978-94-017-2087-8

[26] Blankenship RE. Molecular Mechanisms of Photosynthesis. 2nd ed. John Wiley & Sons; 2014. 314 p. DOI: 10.1002/9780470758472

[27] Granéli E, Turner JT, editors. Ecology of Harmful Algae. Berlin: Springer Science & Business Media; 2006. 406 p. DOI: 10.1007/978-3-540-32210-8

[28] Suggett DJ, Borowitzka MA, Prášil O, editors. Chlorophyll a Fluorescence in Aquatic Sciences: Methods and Applications, Developments in Applied Phycology. Vol. 4. Dordrecht, The Netherlands: Springer; 2010. 326 p. DOI: 10.1007/978-90-481-9268-7

[29] Ke B. Photosynthesis: Photobiochemistry and photobiophysics. In: Govindjee S, editor. Advances in Photosynthesis. Vol. 10. Dordrecht: Kluwer Academic Publishers; 2001. 763 p. DOI: 10.1007/0-306-48136-7

[30] Staehelin LA, Arntzen CJ, editors. Photosynthesis III: Photosynthetic Membranes and Light Harvesting Systems, Encyclopedia of Plant Physiology. Vol. 19. Berlin: Springer; 1986. 802 p. DOI: 10.1007/978-3-642-70936-4

[31] Whitton BA. Diversity, ecology, and taxonomy of the cyanobacteria. In: Mann NH, Carr NG, editors. Photosynthetic Prokaryotes. New York: Plenum Press; 1992. pp. 1-51. DOI: 10.1007/978-1-4757-1332-9_1

[32] Wehrmeyer W. Phycobilisomes: Structure and function. In: Wiessner W, Robinson DG, Starr RC, editors. Cell Walls and Surfaces, Reproduction, Photosynthesis. Experimental Phycology, I. Berlin:Springer; 1990. p. 158-172. DOI:10.1007/978-3-642-48652-4_12

[33] Gantt E. Phycobilisomes. Annual Review of Plant Physiology. 1981;**32**(1):327-347. DOI: 10.1146/annurev.pp.32.060181.001551

[34] Glazer AN. Phycobilisome—A macromolecular complex optimised for light energy transfer. Biochimica et Biophysica Acta. 1984;**768**:29-51. DOI: 10.1016/0304-4173(84)90006-5

[35] MacColl R. Cyanobacterial phycobilisomes. Journal of Structural Biology. 1998;**124**(2-3):311-334. DOI: 10.1006/jsbi.1998.4062

[36] Förster T. Delocalized excitation and excitation transfer. In: Sinanoglu O, editor. Modern Quantum Chemistry Istanbul Lectures. Vol. 3. New York: Academic Press; 1965. pp. 93-137

[37] Şener M, Strümpfer J, Hsin J, Chandler D, Scheuring S, Hunter CN, et al. Förster energy transfer theory as reflected in the structures of photosynthetic light-harvesting systems. Chemphyschem. 2011;**12**(3):518-531. DOI: 10.1002/cphc.201000944

[38] Sauer K. Primary events and the trapping of energy. In: Govindjee S, editor. Bioenergetics of Photosynthesis. London, New York: Academic Press; 1975. pp. 115-181

[39] Mullineaux CW. Phycobilisome-reaction centre interaction in cyanobacteria. Photosynthesis Research. 2008;**95**(2-3):175-182. DOI: 10.1007/s11120-007-9249-y

[40] Wolf E, Schussler A. Phycobiliprotein fluorescence of Nostoc punctiforme changes during the life cycle and chromatic adaptation: Characterization by spectral confocal laser scanning microscopy and spectral unmixing. Plant, Cell and Environment. 2005;**28**(4):480-491. DOI: 10.1111/j.1365-3040.2005.01290.x

[41] Murton J, Nagarajan A, Nguyen AY, Liberton M, Hancock HA, Pakrasi HB, et al. Population-level coordination of pigment response in individual cyanobacterial cells under altered nitrogen levels. Photosynthesis Research. 2017;**134**(2):165-174. DOI: 10.1007/s11120-017-0422-7

[42] Vermaas WF, Timlin JA, Jones HD, Sinclair MB, Nieman LT, Hamad SW, et al. In vivo hyperspectral confocal fluorescence imaging to determine pigment localization and distribution in cyanobacterial cells. Proceedings of the National Academy of Sciences. 2008;**105**(10):4050-4055. DOI: 10.1073/pnas.0708090105

[43] Majumder EL, Wolf BM, Liu H, Berg RH, Timlin JA, Chen M, et al. Subcellular pigment distribution is altered under far-red light acclimation in cyanobacteria that contain chlorophyll f. Photosynthesis Research. 2017;**134**(2):183-192. DOI: 10.1007/s11120-017-0428-1

[44] Nozue S, Katayama M, Terazima M, Kumazaki S. Comparative study of thylakoid membranes in terminal heterocysts and vegetative cells from two cyanobacteria, Rivularia M-261 and *Anabaena variabilis*, by fluorescence and absorption spectral microscopy. Biochimica et Biophysica Acta

(BBA)-Bioenergetics. 2017;**1858**(9):742-749. DOI: 10.1016/j.bbabio.2017.05.007

[45] Ying L, Huang X, Huang B, Xie J, Zhao J, Sheng Zhao X. Fluorescence emission and absorption spectra of single Anabaena sp. strain PCC7120 cells. Photochemistry and Photobiology. 2002;**76**(3):310-313. DOI:10.1562/0031-8655(2002)0760310feaaso2.0.co2

[46] Kumazaki S, Hasegawa M, Ghoneim M, Shimizu Y, Okamoto K, Nishiyama M, et al. A line-scanning semi-confocal multi-photon fluorescence microscope with a simultaneous broadband spectral acquisition and its application to the study of the thylakoid membrane of a cyanobacterium Anabaena PCC7120. Journal of Microscopy. 2007;**228**(2):240-254. DOI: 10.1111/j.1365-2818.2007.01835.x

[47] Millach L, Obiol A, SolÉ A. Esteve I. A novel method to analyse in vivo the physiological state and cell viability of phototrophic microorganisms by confocal laser scanning microscopy using a dual laser. Journal of Microscopy. 2017;**268**(1):53-65. DOI: 10.1111/jmi.12586

[48] Mullineaux CW. FRAP analysis of photosynthetic membranes. Journal of Experimental Botany. 2004;**55**(400):1207-1211. DOI: 10.1093/jxb/erh106

[49] Mullineaux CW, Tobin MJ, Jones GR. Mobility of photosynthetic complexes in thylakoid membranes. Nature. 1997;**390**(6658):421-424. DOI: 10.1038/37157

[50] Liu LN, Aartsma TJ, Thomas JC, Zhou BC, Zhang YZ. FRAP analysis on red alga reveals the fluorescence recovery is ascribed to intrinsic photoprocesses of phycobilisomes than large-scale diffusion. PLoS One. 2009;**4**(4):e5295. DOI: 10.1371/journal.pone.0005295

[51] Vitali M, Reis M, Friedrich T, Eckert HJ. A wide-field multi-parameter FLIM and FRAP setup to investigate the fluorescence emission of individual living cyanobacteria. In: Proceedings of SPIE, Laser Applications in Life Sciences, 9-10 June 2010, Oulu, Finland. Vol. 7376. Finland: International Society for Optics and Photonics; 2010. pp. 737610-737610-6. DOI: 10.1117/12.871520

[52] Yang S, Su Z, Li H, Feng J, Xie J, Xia A, et al. Demonstration of phycobilisome mobility by the time-and space-correlated fluorescence imaging of a cyanobacterial cell. Biochimica et Biophysica Acta (BBA)—Bioenergetics. 2007;**1767**(1):15-21. DOI: 10.1016/j.bbabio.2006.11.012

[53] Blackwell M, Gibas C, Gygax S, Roman D, Wagner B. The plastoquinone diffusion coefficient in chloroplasts and its mechanistic implications. Biochimica et Biophysica Acta (BBA)—Bioenergetics. 1994;**1183**(3):533-543. DOI: 10.1016/0005-2728(94)90081-7

[54] Drepper F, Carlberg I, Andersson B, Haehnel W. Lateral diffusion of an integral membrane protein: Monte Carlo analysis of the migration of phosphorylated light-harvesting complex II in the thylakoid membrane. Biochemistry. 1993;**32**(44):11915-11922. DOI: 10.1021/bi00095a022

[55] Borlinghaus R. Colours count: How the challenge of fluorescence was solved in confocal microscopy. Modern research and educational topics in microscopy. In: Méndez-Vilas A, Díaz J, editors. Colours Count: How the Challenge of Fluorescence was Solved in Confocal Microscopy. Spain: FORMATEX; 2007. pp. 890-899. DOI:10.1.1.564.5122

[56] Li D, Shao L, Chen BC, Zhang X, Zhang M, Moses B, et al. Extended-resolution structured illumination imaging of endocytic and cytoskeletal

dynamics. Science. 2015;**349**:6251, aab3500. DOI: 10.1126/science.aab350

[57] van de Linde S, Heilemann M, Sauer M. Live-cell super-resolution imaging with synthetic fluorophores. Annual Review of Physical Chemistry. 2012;**63**:519-540. DOI: 10.1146/annurev-physchem-032811-112012